

# Slit spectroscopy of nine new $z > 3$ southern QSOs: Damped Ly $\alpha$ and Lyman-limit systems\*

S. Lopez<sup>1</sup>, J. Maza<sup>1</sup>, J. Masegosa<sup>2</sup>, and I. Marquez<sup>2</sup>

<sup>1</sup> Departamento de Astronomía, Universidad de Chile, Casilla 36-D, Santiago, Chile

<sup>2</sup> Instituto de Astrofísica de Andalucía, C/Camino Bajo de Huetor 24, 18080 Granada, Spain

Received 27 July 2000 / Accepted 14 November 2000

**Abstract.** We present  $FWHM = 5$  to  $8 \text{ \AA}$  optical spectra of nine previously unknown quasars (QSOs) drawn from the Calan/Tololo Survey. We have chosen this sample based on QSO redshift,  $z > 3$ , and the presence of either candidate damped Ly $\alpha$  (DLA) or Lyman-limit (LL) systems in their spectra. The spectra show at least 9 DLA systems at redshifts  $2.25 < z < 3.26$ , which are identified by the shape and strength of the H I-Ly $\alpha$  absorption line, by the presence of Ly $\beta$  and low-ionization metal lines at the same redshift, and – in most cases – by the observed Lyman-break. We thus provide the astronomical community with new interesting targets for high resolution spectroscopy on large telescopes. We describe all the spectra with emphasis on the most outstanding DLA and LL systems found.

**Key words.** cosmology: observations – quasars: individual: CTQ 247, CTQ 298, CTQ 314, CTQ 325, CTQ 408, CTQ 460, CTQ 476, CTQ 1005, CTQ 1061 – quasars: general – absorption lines

## 1. Introduction

The use of QSOs as background sources for the study of the absorption systems present in their spectra has proven to be the most sensitive method to detect baryonic gas in the high-redshift Universe. High resolution ( $FWHM \sim 6 \text{ km s}^{-1}$ ) spectra taken with 10 m-class telescopes allow one to probe the diffuse absorbing gas from H I column densities of  $N(\text{H I}) \sim 10^{11} \text{ cm}^{-2}$  of the intergalactic medium to H I column densities of  $N(\text{H I}) \sim 10^{22} \text{ cm}^{-2}$  of the interstellar medium of high- $z$  galaxies, over a significant fraction of the Hubble time.

The relevant technical information to make such studies feasible is the amount of QSO flux that remains unabsorbed in its path to the telescope. Indeed, already at low resolution ( $FWHM \sim 300 \text{ km s}^{-1}$ ) one is able to identify unambiguously at least those absorption systems at the dense limit of the H I column density scale: Lyman-limit (LL) systems, with  $N(\text{H I}) \sim 10^{16} - 10^{19} \text{ cm}^{-2}$ , which probably arise in gas associated with galactic halos (e.g., Lanzetta et al. 1996), and damped Ly $\alpha$  (DLA) systems, with  $N(\text{H I}) \gtrsim 10^{20} \text{ cm}^{-2}$ . The latter are similar column

densities as found in neutral clouds of the Milky Way, a reason to believe that high- $z$  DLA systems are the probable progenitors of present-day galaxies (e.g., Wolfe 1993). If DLA systems trace most of the neutral gas content in the high redshift Universe, they can also be used to trace the evolution of star-forming galaxies through the cosmological mass density  $\Omega_{\text{DLA}}$  (Rao & Turnshek 2000; Storrie-Lombardi & Wolfe 2000) and metallicity  $Z$  (Prochaska & Wolfe 1999).

In this Paper we present 9 new  $FWHM = 5$  to  $8 \text{ \AA}$  QSO spectra that show strong evidence for the presence of either LL or DLA systems. The targets were drawn from the sub-sample of  $z > 3$  QSOs discovered in the course of the Calan/Tololo Survey (CTS). The CTS (Maza et al. 1993) is an objective prism survey of  $16 < B < 20$  southern QSOs. To date, 500 QSOs have been published (Maza et al. 1996, and references therein), 400 have been confirmed (not yet published) and a large number of candidates still await for follow-up spectroscopy. Although no completeness studies have been presented yet, three important differences between the CTS and similar surveys are worth mentioning: the exposure times of 90 min are relatively high, the prism dispersion is low ( $180 \text{ nm}$  at H $\beta$ ), and the QSO candidate selection is made by-eye. These features translate into a very faint magnitude limit of  $B \sim 20$  (the Hamburg/ESO Survey, as an example, reaches  $B = 18 \pm 0.5$ ; Reimers et al. 1997). In addition, the candidate selection by-eye using a  $12\times$  microscope

Send offprint requests to: S. Lopez,  
e-mail: slopez@das.uchile.cl

\* Based on observations made at the European Southern Observatory, La Silla, Chile, and at the Cerro Tololo Interamerican Observatory, Chile, which is operated by AURA, Inc.

**Table 1.** Summary of observed targets

Target	$\alpha_{2000}$	$\delta_{2000}$	$m_B$ <sup>1</sup>	$z$	Tel. + Inst.	Grating/Grism	$FWHM$ [Å]
CTQ 408	00 41 31.49	-49 36 12.4	17.5	3.24	Blanco + R-C	KPGL2	5.7
CTQ 247	04 07 18.01	-44 10 29.7	17.6	3.02	Blanco + R-C	KPGL2	5.7
CTQ 1061	10 48 56.73	-16 37 09.5	17.7	3.37	1.52 m + B&C	#15	7.8
CTQ 1005	01 37 54.49	-27 07 35.8	18.6	3.21	1.52 m + B&C	#15	7.8
CTQ 460	10 39 09.51	-23 13 25.7	17.8	3.13	3.60 m + EFOSC2	#7	5.2
CTQ 314	12 35 45.98	-30 50 52.9	18.7	3.13	3.60 m + EFOSC2	#7	5.2
CTQ 476	14 56 49.83	-19 38 52.0	18.5	3.16	3.60 m + EFOSC2	#7	5.2
CTQ 325	13 42 58.90	-13 55 59.9	18.3	3.20	3.60 m + EFOSC2	#7	5.2
CTQ 298	11 13 50.59	-15 33 33.7	18.7	3.37	3.60 m + EFOSC2	#7	5.2

<sup>1</sup> Blue filter magnitudes from the Digitized Sky Survey.

allows one to detect Ly $\alpha$  down to the IIIaJ plate red limit at  $\lambda \simeq 530$  nm; this translates into a redshift upper limit for the CTS of  $z \simeq 3.37$ . Seven of the QSOs that we present here have already been published by the CTS (though no spectra were shown; see Maza et al. 1995 and references therein), while the other two are new discoveries.

## 2. Observations and data reduction

The spectra were obtained at three different telescopes (see Table 1).

CTQ 408 and CTQ 247 were observed at the CTIO Blanco 4 m telescope on the night of October 8 1999. The R-C grating spectrograph at the  $f/7.8$  R-C focus equipped with grating KPGL-2 and a LORAL  $3K \times 1K$  CCD were used. This configuration yields a dispersion of  $1.9 \text{ \AA}/\text{pixel}$  and a wavelength coverage in first order of  $[3300, 8700] \text{ \AA}$ . Total exposure time was 2700 sec for each object. A slit width of  $1''.5$  was used for the two objects at a typical seeing of  $1''.2$ .

CTQ 1061 and CTQ 1005, originally selected as candidates for H II galaxies, were identified as high redshift QSOs during an observing run executed between January 28 and 30 1998 using the Boller & Chivens spectrograph on the ESO 1.52 m telescope. Grating #15 and a  $2688 \times 512$  pixel LORAL CCD were used. This configuration gives a dispersion of  $3.9 \text{ \AA}/\text{pixel}$  and a wavelength coverage of  $[3500, 10500] \text{ \AA}$ . Total exposure time was 1800 sec for each object. The seeing was  $1''.5$ – $2''.0$ .

CTQ 460, CTQ 298, CTQ 314, CTQ 325, and CTQ 476 were observed as part of an ongoing Survey of DLA systems (see Sect. 4). On the night of April 8 2000 we used Grism #7 of EFOSC2 on the ESO 3.6 m telescope, a configuration that provided a resolution of  $FWHM = 5.2 \text{ \AA}$  and spectral coverage  $[3200, 5200] \text{ \AA}$ . Total exposure times ranged between 1200 and 2400 sec. The seeing ranged between  $1''.3$  and  $2''.3$ .

After bias-subtracting and flat-fielding, all spectra were extracted using an algorithm that attempts to

reduce the statistical noise to a minimum. Briefly stated, the seeing profile is fitted with a Gaussian curve twice. In the first fit all three parameters – width, amplitude and offset from a previously defined position – are free, while in the second fit only the amplitudes are allowed to vary, with width and offset held fixed at values found by a  $\kappa\sigma$ -clipping fit along the dispersion direction to the values obtained in the first step. The same procedure was applied to the spectra of standard stars to correct for the instrument response and to convert counts to flux units. The slit was oriented along the parallactic angle during each observation, so no chromatic effects are expected; however, since the nights were in general non-photometric and relatively narrow slits were used, the present spectra must be considered non-spectrophotometric.

To derive line parameters each spectrum was normalized by a continuum that was defined using cubic splines over featureless spectral regions. Tables 2 to 10 provide a list of identified metal lines, along with observed equivalent-width estimates  $W_{\text{obs}}$  and redshifts. These parameters resulted from Gaussian fits to the lines in the normalized spectra. Central wavelengths are accurate to better than  $0.1 \text{ \AA}$ , and  $W_{\text{obs}} > 5\sigma_W$  for all listed lines.

## 3. Notes on individual spectra

### 3.1. CTQ 408, $z = 3.24$

There are at least four interesting absorption line systems present in the spectrum of CTQ 408.

An associated system (i.e., with absorption redshift  $z_{\text{abs}} \approx z_{\text{em}}$ ) at  $z = 3.231$  is seen in C IV and H I. As commonly found in such systems the high ionization species, here represented by C IV, appear blue-shifted with respect to the QSO systemic velocity (Tytler & Fan 1992).

A DLA system at  $z = 2.248$  is detected through the DLA line at  $\lambda \sim 3948 \text{ \AA}$  and the corresponding Ly $\beta$  line at  $3332 \text{ \AA}$ . The identification is supported by the presence of Al II  $\lambda 1670$  and Fe II  $\lambda 2382$  at the same redshift.

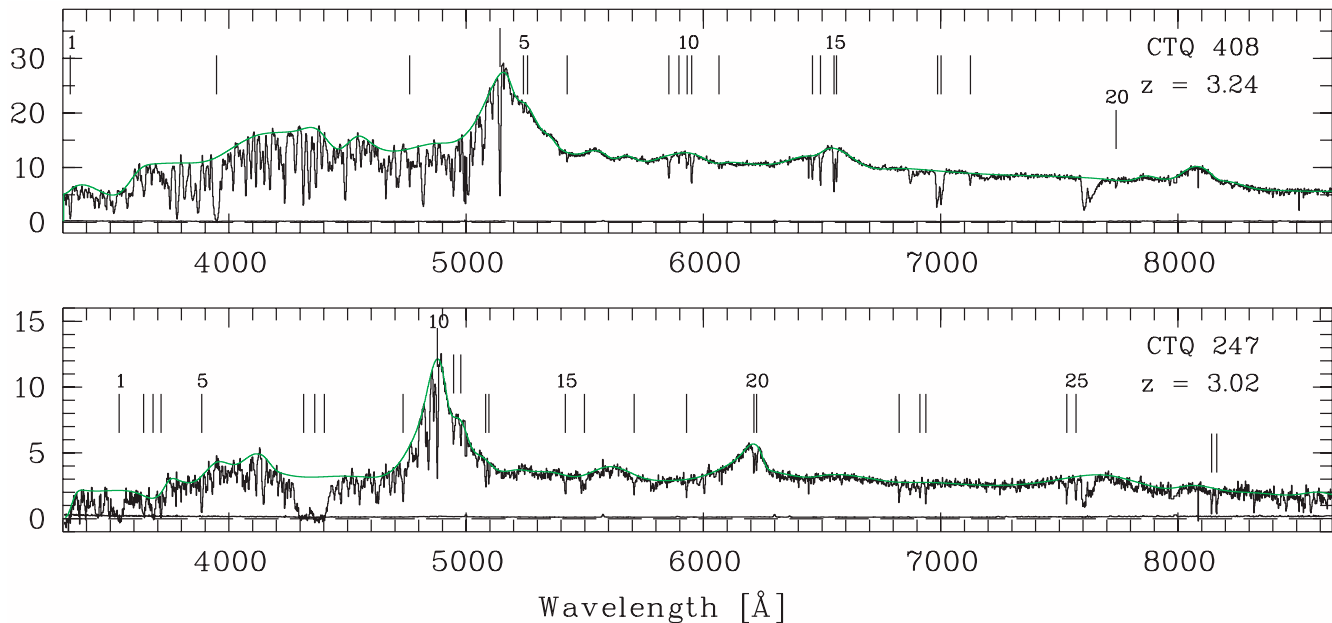


**Fig. 1.** R-C spectra showing outstanding absorption systems described in the text. The smoothed curve indicates the fitted continuum and the lower curve  $1\sigma$  flux errors. The spectral resolution is  $FWHM = 5.7 \text{ \AA}$  and the flux scale is in  $10^{-16} \text{ erg s}^{-1} \text{ cm}^{-2} \text{ \AA}^{-1}$  units

**Table 2.** Identified metal absorption lines in CTQ 408

Line	$\lambda_{\text{obs}}$ [Å]	$W_{\text{obs}}$ [Å]	ID	$z$
1	3331.6	9.12	H I $\lambda 1025$	2.2481
2	3948.2	34.60	H I $\lambda 1215$	2.2478
3	4761.7	3.65	H I $\lambda 1215$	2.9169
4	5142.2	7.39	H I $\lambda 1215$	3.2299
5	5241.6	0.67	N V $\lambda 1238$	3.2311
6	5259.0	0.68	N V $\lambda 1242$	3.2315
7	5425.9	0.97	Al II $\lambda 1670$	2.2475
8	5854.1	2.79	Fe II $\lambda 2344$	1.4973
9	5896.7	0.69	Si IV $\lambda 1393$	3.2308
10	5931.5	2.09	Fe II $\lambda 2374^1$	1.4980
11	5950.6	3.57	Fe II $\lambda 2382$	1.4973
12	6065.4	0.53	C IV $\lambda 1548$	2.9177
13	6459.1	2.45	Fe II $\lambda 2586$	1.4971
14	6493.3	3.28	Fe II $\lambda 2600$	1.4973
15	6550.2	4.01	C IV $\lambda 1548$	3.2311
16	6560.7	3.01	C IV $\lambda 1550$	3.2306
17	6986.9	11.10	Mg II $\lambda 2796$	1.4986
18	7001.7	7.38	Mg II $\lambda 2803$	1.4975
19	7124.7	1.62	Mg I $\lambda 2852$	1.4973
20	7739.1	1.19	Fe II $\lambda 2382$	2.2479

<sup>1</sup> Line blended with Si IV  $\lambda 1402$  at  $z = 3.231$ .

In addition, there is a strong Mg II system at  $z = 1.498$  that also shows absorption by Fe II  $\lambda\lambda 2344, 2374, 2382, 2586$  and  $2600$ , and Mg I  $\lambda 2852$ . The

strength of the Mg II doublet and Fe II lines and the presence of Mg I strongly suggest these lines also arise in a DLA system.

Maybe the most interesting system in the spectrum of CTQ 408 is the optically thin LL system observed at  $z = 2.917$ . Our spectrum shows the corresponding Ly $\alpha$  line along with a weak ( $W_0(\lambda 1548) \sim 0.14 \text{ \AA}$ ) C IV doublet. The interesting point here is that the Lyman break at  $3600 \text{ \AA}$  is steep; together with the fact that the corresponding C IV absorption is weak, the steepness of the break leads us to believe that this LL system has a simple velocity structure. Moreover, simulating the shape of the break as the sum of Voigt profiles accounting for the higher-order Lyman series lines shows that a small H I Doppler parameter,  $b_{\text{HI}} \lesssim 30 \text{ km s}^{-1}$ , reproduces the data better than higher values do. These two properties – lack of multiple velocity components and small  $b$ -value – make of this system a serious candidate for measuring the deuterium-to-hydrogen abundance ratio, D/H. Such a measurement in high-resolution spectra is in general a difficult task because DI is nearly 5 orders of magnitude weaker than H I and the Lyman series absorption lines are separated by only  $82 \text{ km s}^{-1}$ . Thus, there is a rather small range of suitable H I column densities for which the detection *and* profile fit of DI Ly $\alpha$  is possible, with lower limits imposed by the spectrum  $S/N$  and upper limits imposed by saturation of the H I-Ly $\alpha$  line. In this regard, CTQ 408 again appears as a good candidate, given the substantial flux in the region of Ly $\alpha$  absorption,  $F_\lambda \sim 1 \cdot 10^{-15} \text{ erg s}^{-1} \text{ cm}^{-2} \text{ \AA}^{-1}$ , and the small column density of the  $z = 2.917$  LL system,  $N(\text{H I}) = 10^{17.0} \text{ cm}^{-2}$ , as derived from the optical depth at the Lyman break.

**Table 3.** Identified metal absorption lines in CTQ 247

Line	$\lambda_{\text{obs}}$ [Å]	$W_{\text{obs}}$ [Å]	ID	$z$
1	3537.2	17.50	H I $\lambda$ 1215	1.9098
2	3640.4	15.70	H I $\lambda$ 1025	2.5491
3	3680.4	18.70	H I $\lambda$ 1025	2.5881
4	3714.2	9.70	H I $\lambda$ 1025	2.6211
5	3885.7	8.43	C II $\lambda$ 1334	1.9117
6	4314.5	131.98 <sup>1</sup>	H I $\lambda$ 1215	2.5491
7	4362.0	...	H I $\lambda$ 1215	2.5881
8	4402.1	...	H I $\lambda$ 1215	2.6211
9	4734.0	8.32	C II $\lambda$ 1334	2.5473
10	4878.3	6.18	H I $\lambda$ 1215	3.0128
11	4947.2	1.92	Si IV $\lambda$ 1393	2.5495
12	4977.5	1.33	Si IV $\lambda$ 1402	2.5484
13	5082.3	3.43	C IV $\lambda$ 1548?	2.2828
14	5096.0	2.18	C IV $\lambda$ 1550?	2.2861
15	5417.9	3.34	Si II $\lambda$ 1526	2.5487
16	5498.5	5.74	C IV doublet	2.5486
17	5707.6	4.80	Fe II $\lambda$ 1608	2.5485
18	5929.0	2.57	Al II $\lambda$ 1670	2.5486
19	6213.0	2.70	C IV $\lambda$ 1548	3.0130
20	6223.8	2.39	C IV $\lambda$ 1550	3.0133
21	6825.1	3.81	Fe II $\lambda$ 2344	1.9115
22	6912.3	3.06	Fe II $\lambda$ 2374	1.9111
23	6937.1	3.12	Fe II $\lambda$ 2382	1.9114
24	7531.1	4.81	Fe II $\lambda$ 2586	1.9115
25	7569.9	4.53	Fe II $\lambda$ 2600	1.9113
26	8141.8	5.32	Mg II $\lambda$ 2796	1.9116
27	8163.1	6.70	Mg II $\lambda$ 2803	1.9118

<sup>1</sup> Equivalent width estimate of whole absorption feature.

### 3.2. CTQ 247, $z = 3.02$

CTQ 247 is an exceptional line of sight as at least three DLA systems can be seen in its spectrum. The broad trough centered at  $\lambda \sim 4350$  Å can be identified with three DLA lines corresponding to redshifts  $z = 2.55$ , 2.59 and 2.62. This triple identification is supported by the presence of the corresponding Ly $\beta$  lines (lines 2, 3, and 4 in the bottom panel of Fig. 1). Absorption at  $z = 2.55$  is also observed by the low-ionization species C II, Fe II, Al II, and Si II, and by the high-ionization species C IV and Si IV. The large velocity span of  $\sim 6000$  km s<sup>-1</sup> implied by the difference in redshift,  $\Delta z = 0.072$ , is difficult to explain on the basis of a virialized galaxy cluster. If, instead,  $\Delta z$  is due to the Hubble flow, the systems would cover a proper radial distance of  $\sim 18$  Mpc ( $\Omega_0 = 1$ ,  $\Omega_\Lambda = 0$ ,  $H_0 = 50$  km s<sup>-1</sup>/Mpc), i.e., consistent with supercluster size scales. We discuss further this system in Sect. 4.

There is possibly another DLA line at  $\lambda = 3537$  Å corresponding to  $z = 1.91$ . Its DLA nature is supported

**Table 4.** Identified metal absorption lines in CTQ 1061

Line	$\lambda_{\text{obs}}$ [Å]	$W_{\text{obs}}$ [Å]	ID	$z$
1	4952.5	27.80	H I $\lambda$ 1215	3.0739
2	6311.8	5.24	C IV doublet	3.0735

**Table 5.** Identified metal absorption lines in CTQ 1005

Line	$\lambda_{\text{obs}}$ [Å]	$W_{\text{obs}}$ [Å]	ID	$z$
1	3897.8	15.01	H I $\lambda$ 1025	2.8001
2	4622.5	81.00	H I $\lambda$ 1215	2.8025
3	4955.9	16.23	H I $\lambda$ 1215	3.0767
4	5072.8	18.37	C II $\lambda$ 1334	2.8016
5	6315.9	6.90	C IV doublet <sup>1</sup>	3.0762

<sup>1</sup> C IV lines appear blended. Total equivalent width is quoted.

by strong Mg II, Fe II, and C II absorption at the same redshift.

In addition, a  $z_{\text{abs}} \approx z_{\text{em}}$  absorption system is observed at  $z = 3.01$  in Ly $\alpha$  and C IV, that is likely to be responsible for the apparent Lyman-break observed at  $\sim 3700$  Å.

### 3.3. CTQ 1061, $z = 3.37$

The most prominent system in the spectrum of CTQ 1061 is a thick LL system at  $z = 3.07$  (Ly $\alpha$  and an associated C IV doublet are observed), producing the Lyman break observed at 3700 Å. Note that the Ly $\alpha$  line does not reach zero flux at its core, yet being unusually broad. This means this system is probably not damped, but instead it must be made of several velocity components with lower column densities.

### 3.4. CTQ 1005, $z = 3.21$

The spectrum of CTQ 1005 shows a broad trough at  $\lambda = 4623$  Å, which we interpret as a DLA line corresponding to  $z = 2.80$ . The interpretation is supported by the strong line at 3898 Å, identified with Ly $\beta$ , and by C II  $\lambda$ 1334 at the same redshift.

We also find a C IV doublet at  $z = 3.08$ , which is likely to be responsible for the apparent Lyman break at  $\lambda \sim 3750$  Å.

### 3.5. CTQ 460, $z = 3.13$

The spectrum of CTQ 460 shows a broad absorption trough at  $\lambda = 4591$  Å, which we identify with a DLA system at  $z = 2.78$ , also showing Ly $\beta$  and C III  $\lambda$ 977. The Lyman break observed at  $\lambda \sim 3500$ , however, is not consistent with this redshift and must be produced by a LL system at a slightly higher redshift, for which line 7 is a good Ly $\alpha$  candidate.

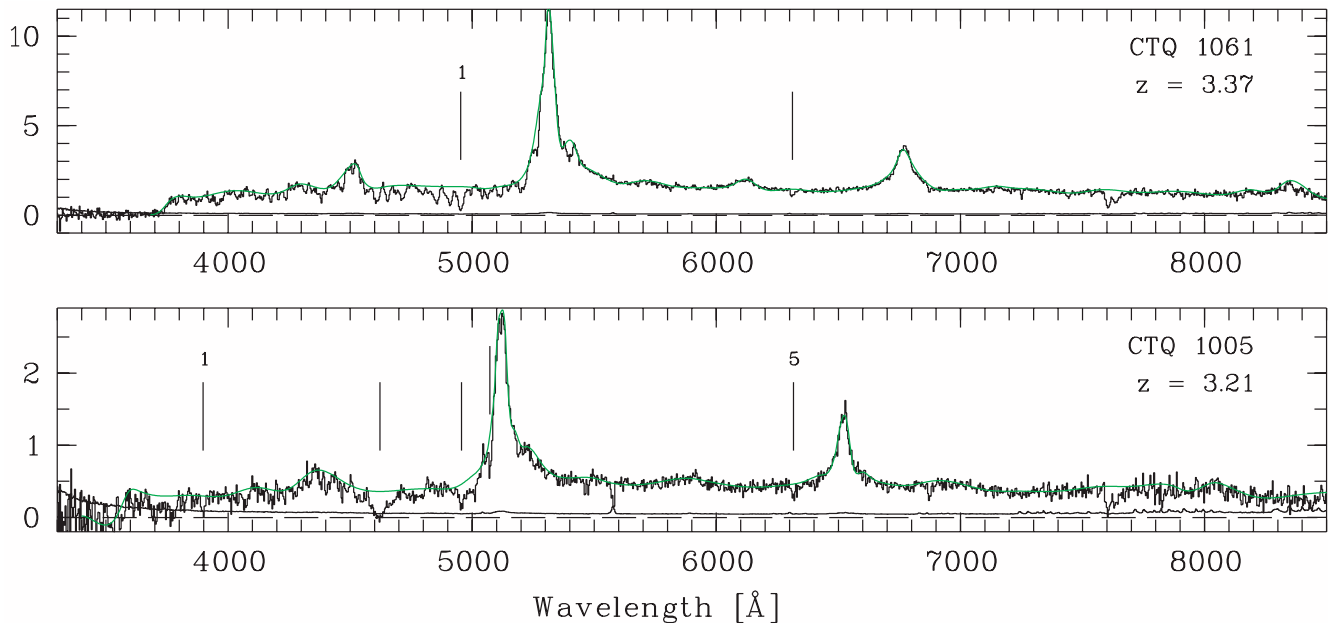


**Fig. 2.** B&C spectra showing outstanding absorption systems described in the text. The smoothed curve indicates the fitted continuum and the lower curve  $1\sigma$  flux errors. The spectral resolution is  $FWHM = 7.8 \text{ \AA}$  and the flux scale is in  $10^{-16} \text{ erg s}^{-1} \text{ cm}^{-2} \text{ \AA}^{-1}$  units

**Table 6.** Identified metal absorption lines in CTQ 460

Line	$\lambda_{\text{obs}}$ [ $\text{\AA}$ ]	$W_{\text{obs}}$ [ $\text{\AA}$ ]	ID	$z$
1	3626.3	14.29 <sup>1</sup>	H I $\lambda 1025$	2.5354
2	3689.4	3.27	C III $\lambda 977$	2.7762
3	3873.8	9.20	H I $\lambda 1025$	2.7767
4	4109.7	6.42	H I $\lambda 1025?$	3.0066
5	4292.1	13.52	H I $\lambda 1215$	2.5306
6	4590.8	65.64	H I $\lambda 1215$	2.7763
7	4645.7	7.66	H I $\lambda 1215$	2.8215
8	4867.3	11.73	H I $\lambda 1215?$	3.0038
9	5004.3	2.20	H I $\lambda 1215$	3.1165
10	5040.1	1.92	H I $\lambda 1215?$	3.1459

<sup>1</sup> Blended feature.

In addition, there appear to be two strong  $\text{Ly}\alpha + \text{Ly}\beta$  systems at  $z = 2.53$  and  $z = 3.00$ . Nevertheless, we may ask whether the line identifications for the  $z = 3.00$  system are correct, because, despite the strength of the  $\text{Ly}\alpha$  line (as compared with line 7), no corresponding Lyman break is observed. Concerning the  $z = 2.53$  system, a possible LL break falls in the absorbed part of the spectrum.

There are also two interesting  $z_{\text{abs}} \approx z_{\text{em}}$  systems at  $z = 3.12$  and  $z = 3.15$ , which are observed in  $\text{Ly}\alpha$  (lines 9 and 10) but not in  $\text{Nv}$ . We note, however, that line 10 also matches  $\text{Si II } \lambda 1260$  at  $z = 3.00$ .

### 3.6. CTQ 314, $z = 3.13$

This line of sight again shows two likely  $z_{\text{abs}} \approx z_{\text{em}}$   $\text{Ly}\alpha$  systems at  $z = 3.12$  and  $z = 3.14$ . However, the blue-most  $\text{Ly}\alpha$  component, although stronger, does not have

**Table 7.** Identified metal absorption lines in CTQ 314

Line	$\lambda_{\text{obs}}$ [ $\text{\AA}$ ]	$W_{\text{obs}}$ [ $\text{\AA}$ ]	ID	$z$
1	3587.7	11.39	H I $\lambda 1025$	2.4977
2	4244.3	5.59	H I $\lambda 1025$	3.1394
3	4253.3	7.00	H I $\lambda 1215$	2.4987
4	4269.9	2.88	O VI $\lambda 1032?$	3.1378
5	4294.0	3.28	O VI $\lambda 1037?$	3.1383
6	5011.8	4.03	H I $\lambda 1215?$	3.1227
7	5031.0	2.22	H I $\lambda 1215?$	3.1385

a corresponding  $\text{Ly}\beta$  line, thus making the identification insecure.  $\text{Nv}$  is not detected in neither of the systems but in the  $z = 3.14$  component there is indication for strong O VI absorption (lines 4 and 5).

In addition, lines 1 and 3 match well with  $\text{Ly}\beta$  and  $\text{Ly}\alpha$  at  $z = 2.50$  but the strength and asymmetry of the former line suggest it is blended with another strong  $\text{Ly}\alpha$  line. Alternatively, if line 2 is mainly due to  $\text{Ly}\alpha$ , then the match in total line strength between the blended  $\text{Ly}\alpha$  and  $\text{Ly}\beta$  absorption features is better.

### 3.7. CTQ 476, $z = 3.16$

There is a possible DLA line at  $\lambda = 3854 \text{ \AA}$  (the line is unusually broad, with  $FWHM \approx 22 \text{ \AA}$ , and the flux reaches zero at the line core), but the corresponding  $\text{Ly}\beta$  line falls out of our wavelength range due to a LL system at higher redshift. The same is true for the broad ( $FWHM \approx 14 \text{ \AA}$ ) line at  $\lambda = 4074 \text{ \AA}$ , but here the identification is supported by C II, Si II, and strong C IV absorption at the same redshift.

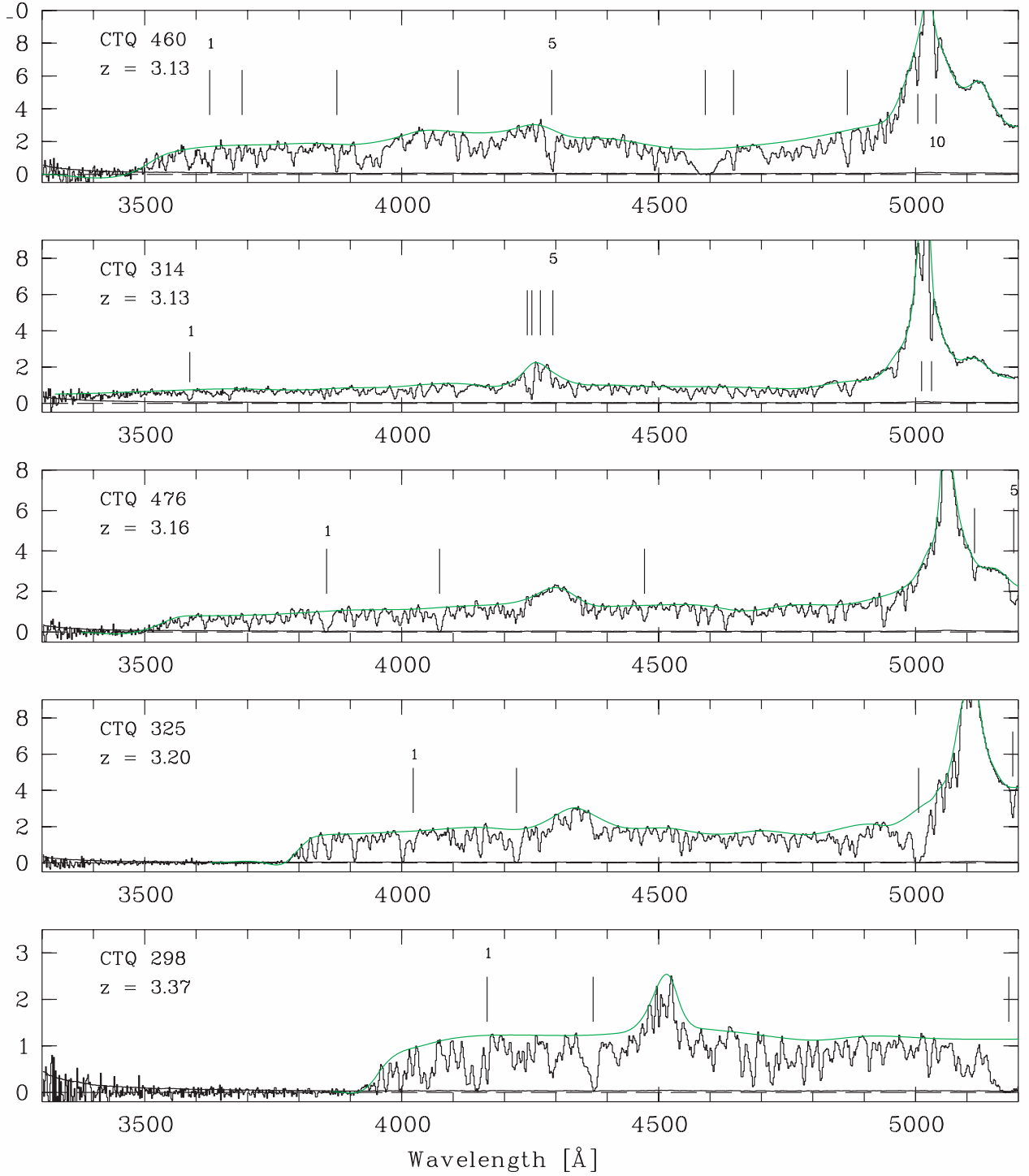


**Fig. 3.** EFOOSC2 spectra of  $z > 3$  QSOs from the ongoing DLA survey. The smoothed curve indicates the fitted continuum and the lower curve  $1\sigma$  flux errors. The spectral resolution is  $FWHM = 5.2 \text{ \AA}$  and the flux scale is in  $10^{-16} \text{ erg s}^{-1} \text{ cm}^{-2} \text{ \AA}^{-1}$  units

### 3.8. CTQ 325, $z = 3.20$

A DLA system is seen at  $z = 3.12$  with  $\text{Ly}\alpha$ ,  $\text{Ly}\beta$ ,  $\text{C III } \lambda 977$ ,  $\text{Si II } \lambda 1260$  and the corresponding Lyman-break clearly identified.

### 3.9. CTQ 298, $z = 3.37$

The spectrum of CTQ 298 shows a DLA system at  $z = 3.26$ , again based on  $\text{Ly}\alpha$ ,  $\text{Ly}\beta$ ,  $\text{C III } \lambda 977$  and the corresponding Lyman-break.

**Table 8.** Identified metal absorption lines in CTQ 476

Line	$\lambda_{\text{obs}}$ [Å]	$W_{\text{obs}}$ [Å]	ID	$z$
1	3853.8	20.61	H I $\lambda$ 1215	2.1701
2	4073.7	15.16	H I $\lambda$ 1215	2.3510
3	4472.6	6.62	C II $\lambda$ 1334	2.3516
4	5114.8	2.00	Si II $\lambda$ 1526	2.3502
5	5191.1	7.13	C IV doublet <sup>1</sup>	2.3502

<sup>1</sup> C IV lines appear blended. Total equivalent width is quoted.

**Table 9.** Identified metal absorption lines in CTQ 325

Line	$\lambda_{\text{obs}}$ [Å]	$W_{\text{obs}}$ [Å]	ID	$z$
1	4022.4	6.67	C III $\lambda$ 977	3.1170
2	4223.5	18.99	H I $\lambda$ 1025	3.1176
3	5005.9	42.26	H I $\lambda$ 1215	3.1178
4	5189.0	2.90	Si II $\lambda$ 1260	3.1178

**Table 10.** Identified metal absorption lines in CTQ 298

Line	$\lambda_{\text{obs}}$ [Å]	$W_{\text{obs}}$ [Å]	ID	$z$
1	4166.2	7.43	C III $\lambda$ 977	3.2643
2	4372.5	24.94	H I $\lambda$ 1025	3.2626
3	5181.4	98.91	H I $\lambda$ 1215	3.2622

#### 4. Summary and discussion

We have presented all 9  $z > 3$  CTS QSOs observed so far at medium resolution ( $FWHM = 5$  to  $8$  Å) that show strong evidence for either a LL or DLA system in their spectra. Based on the strength and shape of the Ly $\alpha$  line, and the presence of Ly $\beta$  and absorption by heavy ions at the same redshift, we detect *unambiguously* 9 DLA systems in 6 lines of sight, with redshifts ranging from  $z = 2.25$  to  $z = 3.26$ . In addition, one of the spectra (CTQ 408) shows a strong low-ionization (Mg II, Mg I, Fe II) metal system, which might be identified with a DLA system at  $z = 1.498$ .

This apparent high incidence of DLA systems can partly be explained by noting that five of the QSOs (CTQ 460, CTQ 314, CTQ 476, CTQ 325, and CTQ 298) were observed as part of an ongoing Survey of DLA systems. The Survey description, its goals and results will be presented in a future paper. Worth mentioning here is that the low-resolution ( $FWHM \sim 20$  Å) follow-up spectra of CTS QSOs have allowed us – based on the *likely* presence of a DLA line – to build up a sub-sample of most probable DLA candidates. Higher resolution ( $\sim 5$  Å) and  $S/N$  ( $\sim 20$ ) spectroscopy of those candidates can be used

to discern, in most cases, between a real DLA line profile and a complex blend of Ly $\alpha$  forest lines. The presence of a corresponding Ly $\beta$  line or outstanding metal lines makes such an identification yet more reliable. Here we have reported all five  $z > 3$  QSOs so far observed using this procedure. Therefore, due to the pre-selection of DLA candidates, it is not surprising that these 5 spectra show 3 DLA systems.

On the other hand, the remaining four QSOs (CTQ 408, CTQ 247, CTQ 1061, and CTQ 1005, all observed prior to begin of the DLA Survey and solely in regard to their high redshift) have been chosen due to the serendipitous presence of either a DLA or LL system in their spectra. Special attention must be paid to CTQ 247 (Sect. 3.2) since its spectrum already shows 4 DLA systems. In particular, the three systems observed at  $z \sim 2.6$  are even more atypical because of their small redshift difference,  $\Delta z = 0.072$ . The a priori probability of finding three DLA systems in such a small redshift range is so low,  $\sim 3 \cdot 10^{-6}$ , that it supports a physical connection between them. Therefore, this line of sight clearly deserves further study: (1) Identification of the putative supercluster of proto-galaxies at the same redshift of the absorbers is now possible with deep mid-IR images on an 8m-class telescope. (2) The possible detection of high-ionization absorbing gas (e.g., via O VI) in a high resolution spectrum of CTQ 247 is important because it would give information on the physical state of the intracluster gas. (3) Concerning the DLA systems themselves, measuring metal abundances in each of the systems would give clues to the chemical evolution of DLA systems; in fact, assuming the absorbers are physically associated, then similar metallicities would be expected, due to similar stellar-evolution histories. (4) Resolved absorption profiles would help test current models on the kinematics of DLA systems by comparing three – or more? – systems that might be dynamically associated. In summary, the 3 DLA systems observed at  $z \sim 2.6$  toward CTQ 247 represent a unique case and can be used as a laboratory for testing models of both galaxy formation and chemical evolution, at a redshift where galactic structures are perhaps still in process of formation.

Finally, let us emphasize that all the absorption systems we have described in this paper deserve further study at high-resolution. The present sample of new QSOs thus enlarges the still scarce number of high- $z$  southern QSOs that are bright enough for high-resolution spectroscopy on 8 m-class telescopes.

*Acknowledgements.* We thankfully acknowledge the important suggestions made by the referee, Dr. S. Savaglio, to improve the clarity of the paper. We have also benefited from helpful discussions with Dr. S. Ellison and Dr. L. F. Barrientos. S. L. acknowledges financial support by FONDECYT grant No. 3000 001 and by the Deutsche Zentralstelle für Arbeitsvermittlung. J. M. acknowledges financial support by FONDECYT grant No. 1 980 172.

**References**

- Lanzetta, K. M., Webb, J. K., & Barcons, X. 1996, ApJ, 456, 17
- Maza, J., Ruiz, M. T., Gonzalez, L. E., Wischnjewsky, M., & Antezana, R. 1993, RMxA&A, 25, 51
- Maza, J., Wischnjewsky, M., Antezana, R., & Gonzalez, L. E. 1995, RMxA&A, 31, 119
- Maza, J., Wischnjewsky, M., & Antezana, R. 1996, RMxA&A, 32, 35
- Prochaska, J. X., & Wolfe, A. M. 1999, ApJS, 121, 369
- Rao, S. M., & Turnshek, D. A. 2000, ApJS, in press [astro-ph/9909164]
- Reimers, D., & Wisotzki, L. 1997, The Messenger, 88, 14
- Storrie-Lombardi, L. J., & Wolfe, A. M. 2000, ApJ, in press [astro-ph/0006044]
- Tytler, D., & Fan, X.-M. 1992, ApJS, 79, 1
- Wolfe, A. M. 1993, Ann. NY Acad. Sci., 668, 281